Design and Development of a Laboratory-scale Ice Adhesion Testing Device

Joseph G. Smith Jr.[1], Christopher J. Wohl[1], Jose Palacios[2], and Bryce D. Connelly[3]
[1]NASA Langley Research Center, Hampton, VA 23681, United States of America
[2]The Pennsylvania State University, University Park, PA 16802, United States of America
[3] Space-X, 1 Rocket Road, McGregor, TX 76657, United States of America
joseph.g.smith@nasa.gov

Introduction

When an aircraft traverses through clouds containing supercooled water droplets, in-flight icing can occur that negatively affects vehicle performance by increasing weight and drag leading to loss of lift. Super-cooled water droplets present in clouds that impact vehicle surfaces can lead to in-flight icing any time during the year.[1] Most events occur at temperatures ranging from 0 to -20°C. Ice generated on the aircraft can vary between clear/glaze, rime, and mixed (Fig. 1) depending on air temperature (-5 to -20°C), liquid water content (0.3-0.6 g/m^3), and droplet size (median volumetric diameter of 15-40 μm).

Clear/Glaze	Mixed	Rime

Figure 1: Types of accreted impact icing

Current strategies to remove ice are based on active technologies such as pneumatic boots, heated surfaces, and deicing agents (i.e., ethylene- and propylene-based glycols). The latter have potential environmental concerns. A passive approach to mitigate accreting ice that is actively being investigated are protective coatings. An ice mitigating coating could potentially be used as a stand-alone material, but more likely in combination with an active approach. In the latter scenario, potential reduction in power consumption by the active approach may be realized.

To determine the ice adhesion strength of impact ice that is representative of the aircraft environment is not a trivial matter. Test methods utilizing slowly formed ice (i.e., freezer ice) do not accurately simulate this environment. Likewise, some testing methodologies involve sample relocation from the icing environment to the test chamber that can result in thermal shock to the sample, thus affecting the results. The Adverse Environment Rotor Test Stand (AERTS) located at Pennsylvania State University (PSU) has been demonstrated to simulate impact icing conditions within the icing envelope for the determination of ice adhesion shear strength (IASS) without removal/relocation of the sample.[2] Due to the confidence in results obtained from AERTS, this instrument is in high demand and requires a significant amount of lead time and capital investment to obtain IASS results. As a solution for quickly and economically screening coatings in a controlled manner under impact icing conditions, a laboratory-scale ice adhesion test device (AERTS Jr., Fig. 2) was developed under contract by PSU for NASA based on AERTS. Details of the device and the IASS of uncoated aluminum (Al) samples are described herein.

Figure 2: AERTS Jr.

Experimental

Ice adhesion shear strength (IASS) of an uncoated aluminum 6061 T6 airfoil (88.87 mm x 12.85 mm x 15.14 mm) was determined at -8, -12, and -16°C in AERTS Jr.. The instrument was controlled by a LabVIEW program developed by PSU that monitored sensors for the tachometer and accelerometer. Temperature within the test section was monitored by a UEI DTK2 differential thermometer. Prior to attachment to opposing sides of the centrifuge rotor, the mass of the live (sample to be tested) and dead (reference to record the mass of ice accreted) blades were determined. The rotor/blade assembly was then secured to a hub within the refrigerated centrifuge and spun at 2500 to 3000 rpm at the desired test temperature for a minimum of 20 min before testing to attain thermal equilibrium. The rotor rpm was subsequently increased to approximately 5600 rpm with water being introduced into the cold chamber through a pneumatically driven NASA MOD 2 nozzle generating a water droplet mean volumetric diameter of 20 μm. As the rotor turned at speed, ice accreted on both blades with subsequent shedding of ice from the live blade that was recorded when ice was released and impacted the ballistic wall. At this time, the water was turned off and the rpm of the rotor/blade assembly brought to zero. The door to the test chamber was then opened and a shield placed in front of the water nozzle to deflect the airflow. The assembly was then removed from the hub and placed on a wire rack within the upper portion of the test chamber. Digital images of the live and dead blades were then taken with a Canon Power Shot ELPH180. The lengths and width of the ice shed area on the live blade were obtained using Starrett 799 digital calipers. The live and dead blades were then removed from the rotor/blade assembly to obtain the final mass. The IASS of the live blade was determined from the difference in mass (before and after testing) of the live and dead blades, the ice shed area, and the rpm of the shed event. The same live blade sample was tested in triplicate at all three test temperatures. Surface roughness was determined using a Bruker Dektak XT Stylus Profilometer. Measurements were conducted using a 12.5 µm tip at a vertical range of 65.5 µm with an applied force of 3 mg. Data were collected over a 1.0 mm length at a resolution of 0.056 µm/point. Five single line scans at different locations were collected and processed using a two-point leveling subtraction. The resultant R_a (arithmetic roughness) and R_q (root mean square roughness) average values were calculated.

Results and Discussion

AERTS Jr.

A schematic of this laboratory scale screening tool is shown in Fig. 3. The main components are 1) a modified refrigerated centrifuge, 2) a freezer compartment with water nozzle, and 3) a water tank. A PSU developed LabVIEW program controls the rotor speed in rpm. An ice shed event is recorded when ice, released from the live blade, impacts the steel ballistic wall.

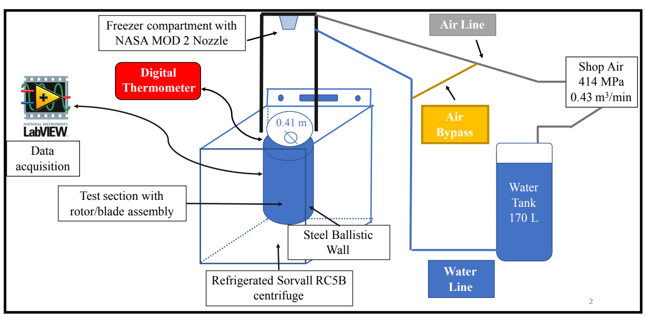

Figure 3: AERTS Jr. schematic

Modifications to a Sorvall RC5B included lining the centrifuge chamber with a steel ballistic wall for impacting ice from a shed event and removal of the door to accommodate a freezer compartment with a NASA MOD 2 nozzle. The centrifuge can attain temperatures of -20°C and speeds of 21,000 rpm. However, in actual operation, speeds are maintained below 6600 rpm based on bolt strength limitations.

Location of the sensors to monitor the shed event and rotor speed within the test section are shown in Fig. 4. An accelerometer attached to the ballistic wall (acting as an on/off switch for monitoring the test in the LabVIEW program) senses the impacting ice from a shed event that is recorded at the shed event rpm. A plexiglass piece fitted with magnets and attached to the rotor hub allowed for rotor speed to be monitored in LabVIEW as the magnets passed in front of a Hall effect sensor. To concentrate the icing cloud generated from water droplets provided by the NASA MOD 2 nozzle onto the test blades and shield the spinning rotor, a spray cover was constructed (Fig. 4). A thermocouple attached to the shield bottom monitors air temperature just above the

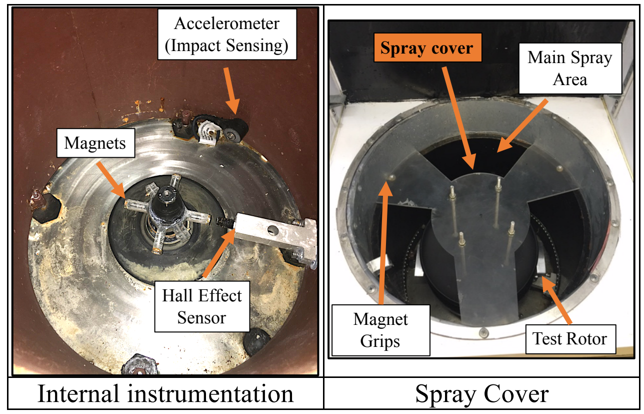

Figure 4: Internal instrumentation and spray cover

spinning blades.

The live and dead blades were attached to the rotor with the assembly (Fig. 5) residing within the test section below the spray cover shield. Spacers inserted between the rotor and blades prevented ice bridging between the two.

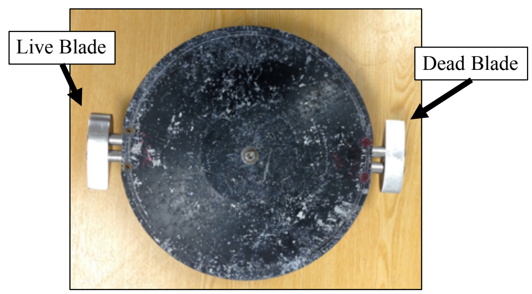

Figure 5: Rotor/blade assembly

The icing cloud was generated using a NASA MOD 2 nozzle that resides in the freezer compartment ceiling. This nozzle is a version of ones used in NASA Glenn's Icing Research Tunnel and has a needle that provides a lower volume flow rate compared to a standard nozzle. It is secured in a casing located in the ceiling where air and water lines are located. The components and assembly are shown in Fig. 6. The nozzle assembly is fitted with air and water pressure transducers that provide data to LabVIEW to determine the mean volume diameter (MVD) of the water droplets generated. This assembly is situated between cooling lines in the freezer compartment so as to keep it cold during operation.

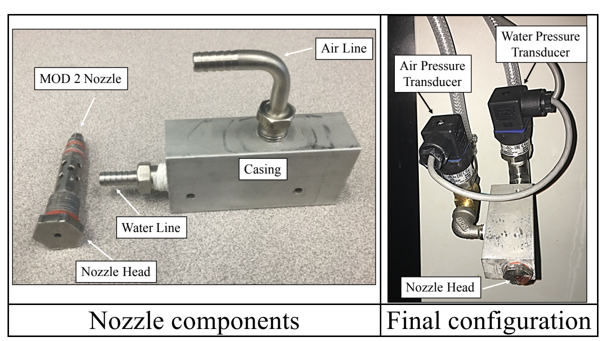

Figure 6: Nozzle assembly

An image of the LabVIEW program (Fig. 7) shows the pressure gauges, rotor rpm, MVD, and shed event rpm that a user needs to obtain the correct test conditions.

Figure 7: LabVIEW program screen

Testing of uncoated Al samples

The IASS of uncoated Al airfoils was determined at -8, -12, and -16°C within the FAR Part 25/29 Appendix C icing envelope.[3] Rotor rotation was between 5500 and 5600 rpm affording a linear velocity (v) of 93.3 to 95.0 m/s as determined by Eqn. 1 where r is the rotor radius in m.

$$v = r * rpm * 0.10472\ s^{-1} \qquad (1)$$

Examples of ice accreted on the dead blade at each temperature is shown in Fig. 8. The difference in mass of the dead and live blades before and after testing afforded the mass of ice shed (m_{ice}) from the live blade. The shed area

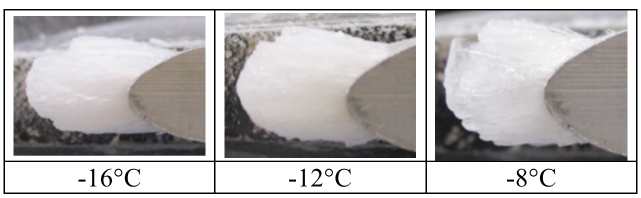

Figure 8: Ice shapes on dead blade

in mm^2 was determined according to Eqn. 2 from measurements [width (W) and H1 - H4] of this area on the live blade as illustrated in Fig. 9.

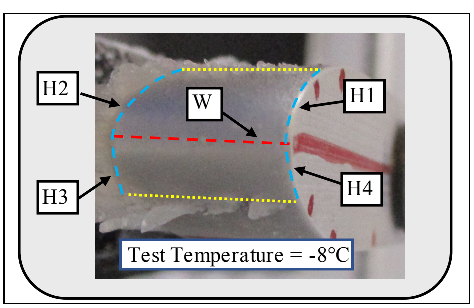

Figure 9: Measurement of ice shed area

$$\text{Shed area} = [W * (H2 + H4)] + [0.5W * (H1 - H2)] + [0.5\ W * (H3 - H4)] \qquad (2)$$

The IASS in N/mm^2 (or MPa) is determined according to Eqn. 3 where m_{ice} is in kg, v is in m/s, and r is in m.

$$IASS = (m_{ice} * v^2)/r \qquad (3)$$

The IASS values for the airfoils were compared to those measured on uncoated Al 3003 panels evaluated in AERTS.[4] R_a and R_q were comparable for the AERTS Jr. airfoils (0.306 and 0.382 µm, respectively) and AERTS panels (0.326 and 0.388 µm, respectively) allowing for direct data comparison. In AERTS, the rotor was operated at 400 rpm (v = 63.84 m/s) in an icing cloud density (i.e., liquid water content, LWC) of 1.9 g/m^3 with a MVD of 20 µm. The LWC is not determined in AERTS Jr. Prior results in AERTS saw an effect of 7% due to the LWC.[2] The IASS for each facility is shown in Table 1. What becomes evident is that the results in AERTS Jr. were approximately 5 to 6 times greater than that in AERTS. This may be due to differences in facilities and operational parameters (v, LWC, rotor type, sample).

Table 1: IASS in kPA

Facility	-16°C	-12°C	-8°C
AERTS	149.4 ± 11.9	97. 6 ± 5.8	64.6 ± 16.6
AERTS Jr.	879.8 ± 78.0	597.8 ± 106.4	299.1 ± 83.1

However, a graph of the average data normalized to the IASS at -16°C (Fig. 10) from both facilities revealed that performance was comparable. The regression line and correlation coefficient are given in the figure.

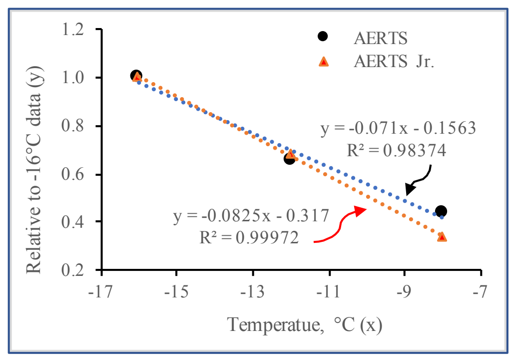

Figure 10: Performance comparison.

Conclusions

A laboratory scale screening tool for IASS was developed. The IASS in AERTS Jr. followed the expected trend of decreasing IASS with increasing temperature. However, AERTS Jr. IASS were approximately 5 to 6 times that of comparable materials examined in AERTS. The relative performance though was comparable.

References

1. M.G. Paotapczuk, *J. Aerosp. Eng.*, 26 (2013) 260-276 and references therein.
2. J. Soltis et al., 54th AIAA/ASME/ASCE/AHS/ASC Structures, Structural Dynamics, & Materials Conference, 2013 Apr 8-11, Boston, MA, AIAA 2013-1509.
3. R.K. Jeck, DOT/FAA/AR-00/30. April 2002.
4. J.G. Smith Jr. et al., 39th Annual Meeting of the Adhesion Society, 2016 Feb 21-24, San Antonio, TX.